\



Pressure tuning of the anomalous Hall effect in the kagome superconductor CsV_3Sb_5

Fang-Hang Yu(喻芳航), Xi-Kai Wen(温茜凯), Zhi-Gang Gui(桂智刚), Tao Wu(吴涛), Zhenyu Wang(王震宇), Zi-Ji Xiang(项子雾), Jianjun Ying(应剑俊), and Xianhui Chen(陈仙辉)

Citation: Chin. Phys. B, 2022, 31 (**1**): 017405. DOI: 10.1088/1674-1056/ac3990
Journal homepage: http://cpb.iphy.ac.cn; http://iopscience.iop.org/cpb

What follows is a list of articles you may be interested in

Evolution of superconductivity and charge order inpressurized RbV_3Sb_5

Feng Du(杜锋), Shuaishuai Luo(罗帅帅), Rui Li(李蕊), Brenden R. Ortiz, Ye Chen(陈晔),Stephen D. Wilson, Yu Song(宋宇), and Huiqiu Yuan(袁辉球)

Chin. Phys. B, 2022, 31 (**1**): 017404. DOI: 10.1088/1674-1056/ac4232

Pressure-induced anomalous insulating behavior in frustrated iridate $La_3Ir_3O_{11}$

Chun-Hua Chen(陈春华), Yong-Hui Zhou(周永惠), Ying Zhou(周颖), Yi-Fang Yuan(袁亦方), Chao An(安超), Xu-Liang Chen(陈绪亮), Zhao-Ming Tian(田召明), and Zhao-Rong Yang(杨昭荣)

Chin. Phys. B, 2021, 30 (**6**): 067402. DOI: 10.1088/1674-1056/abf100

Robust two-gap strong coupling superconductivity associated with low-lying phonon modes in pressurized Nb_5Ir_3O superconductors

Bosen Wang(王铂森), Yaoqing Zhang(张尧卿), Shuxiang Xu(徐淑香), Kento Ishigaki, Kazuyuki Matsubayashi, Jin-Guang Cheng(程金光), Hideo Hosono, Yoshiya Uwatoko

Chin. Phys. B, 2019, 28 (**10**): 107401. DOI: 10.1088/1674-1056/ab4047

Multiband nodeless superconductivity near the charge-density-wave quantum critical point in $ZrTe_{3-x}Se_x$

Shan Cui(崔珊), Lan-Po He(何兰坡), Xiao-Chen Hong(洪晓晨), Xiang-De Zhu(朱相德), Cedomir Petrovic, Shi-Yan Li(李世燕)

Chin. Phys. B, 2016, 25 (**7**): 077403. DOI: 10.1088/1674-1056/25/7/077403

Interplay of superconductivity and d-f correlation in $CeFeAs_{1-x}P_xO_{1-y}F_y$

Luo Yong-Kang, Li Yu-Ke, Wang Cao, Lin Xiao, Dai Jian-Hui, Cao Guang-Han, Xu Zhu-An

Chin. Phys. B, 2013, 22 (**8**): 087415. DOI: 10.1088/1674-1056/22/8/087415

SPECIAL TOPIC — Superconductivity in vanadium-based kagome materials

Pressure tuning of the anomalous Hall effect in the kagome superconductor CsV_3Sb_5

Fang-Hang Yu(喻芳航)[1], Xi-Kai Wen(温茜凯)[1], Zhi-Gang Gui(桂智刚)[1], Tao Wu(吴涛)[1], Zhenyu Wang(王震宇)[1], Zi-Ji Xiang(项子雾)[1], Jianjun Ying(应剑俊)[1,†], and Xianhui Chen(陈仙辉)[1,2,3,‡]

[1] *Hefei National Laboratory for Physical Sciences at Microscale and Department of Physics, and CAS Key Laboratory of Strongly-coupled Quantum Matter Physics, University of Science and Technology of China, Hefei* 230026, *China*

[2] *CAS Center for Excellence in Quantum Information and Quantum Physics, Hefei* 230026, *China*

[3] *Collaborative Innovation Center of Advanced Microstructures, Nanjing* 210093, *China*

(Received 18 October 2021; revised manuscript received 11 November 2021; accepted manuscript online 15 November 2021)

Controlling the anomalous Hall effect (AHE) inspires potential applications of quantum materials in the next generation of electronics. The recently discovered quasi-2D kagome superconductor CsV_3Sb_5 exhibits large AHE accompanying with the charge-density-wave (CDW) order which provides us an ideal platform to study the interplay among nontrivial band topology, CDW, and unconventional superconductivity. Here, we systematically investigated the pressure effect of the AHE in CsV_3Sb_5. Our high-pressure transport measurements confirm the concurrence of AHE and CDW in the compressed CsV_3Sb_5. Remarkably, distinct from the negative AHE at ambient pressure, a positive anomalous Hall resistivity sets in below 35 K with pressure around 0.75 GPa, which can be attributed to the Fermi surface reconstruction and/or Fermi energy shift in the new CDW phase under pressure. Our work indicates that the anomalous Hall effect in CsV_3Sb_5 is tunable and highly related to the band structure.

Keywords: anomalous Hall effect (AHE), charge-density-wave (CDW), kagome superconductor, pressure effect

PACS: 74.62.Fj, 71.18.+y, 71.45.Lr **DOI:** 10.1088/1674-1056/ac3990

1. Introduction

The anomalous Hall effect (AHE), which occurs due to an "anomalous" transverse group velocity of carriers, has been one of the most attractive transport phenomena in the condensed matter physics since its experimental discovery more than a century ago.[1] In general, the AHE can be broadly engendered by two classes of mechanisms: the extrinsic and the intrinsic ones. The extrinsic mechanism owes to spin-dependent impurity scattering effects, including skew-scattering ($\rho_{xy} \propto \rho_{xx}$) and side jump ($\rho_{xy} \propto \rho_{xx}^2$).[2,3] The intrinsic mechanism governed by the electronic structure of a material is related to the nonzero Berry curvature ($\rho_{xy} \propto \rho_{xx}^2$),[4–7] which is the dominant mechanism in topological materials like $Co_3Sn_2S_2$,[8] $ZrTe_5$[9] and GdPtBi.[10] On the other hand, the AHE can be divided into three regimes by the magnitude of conductivity σ_{xx}: dirty limit ($\sigma_{xx} < 10^4$ $(\Omega\cdot\text{cm})^{-1}$), intrinsic dominant ($10^4$ $(\Omega\cdot\text{cm})^{-1} < \sigma_{xx} < 10^6$ $(\Omega\cdot\text{cm})^{-1}$) and clean limit ($\sigma_{xx} > 10^6$ $(\Omega\cdot\text{cm})^{-1}$).[1–3,11,12]

Recently, a new family of topological kagome metals AV_3Sb_5 (A = K, Rb, Cs) have attracted great attention due to their abundant physical properties.[13] These materials possess a layered hexagonal centrosymmetric structure with space group $P6/mmm$ (No. 191). There are two kinds of Sb sites. The vanadium sublattice in the V–Sb1 layers forms an ideal 2D kagome network, and the Sb2 atoms locate between the kagome hexagons and the alkali-metal layers as shown in Fig. 1(a). Interestingly, these compounds show superconductivity with the superconducting transition temperature T_C = 0.93 K, 0.92 K, 2.5 K for A = K, Rb, Cs, respectively.[14–17] In addition, a charge density wave (CDW) order appears below a transition temperature 78–105 K across the three compounds.[13,14,16] Furthermore, unconventional giant AHE was observed in the nonsuperconducting $K_{1-x}V_3Sb_5$ and superconducting CsV_3Sb_5 with the absence of magnetic order or local moments.[18,19] More interestingly, a strong correlation between the AHE and CDW state was revealed in CsV_3Sb_5,[19] which may associate with the unconventional chiral charge order.[20,21] However, the origin of the AHE is still a mystery.

Since the CDW state and the AHE in CsV_3Sb_5 are intimately correlated, it is desirable to further manipulate the AHE and to investigate their relationship. In this regard, pressure can be employed as a clean and effective means, especially for the materials with abundant physical properties like CsV_3Sb_5. In fact, unusual competition between CDW and SC under pressure was reported previously.[22,23] A new CDW order is suggested to appear above 0.7 GPa,[22,23] which may

†Corresponding author. E-mail: yingjj@ustc.edu.cn
‡Corresponding author. E-mail: chenxh@ustc.edu.cn

© 2022 Chinese Physical Society and IOP Publishing Ltd

strongly suppress the superconductivity. More interestingly, a new superconducting dome emerges above 15 GPa without CDW order.[24–27] However, despite a large number of high-pressure works on CsV_3Sb_5, there is no systematic study of the AHE under pressure so far. In addition, many experimental observations of high pressure modulated AHE have been reported in the other topological materials.[28–35] In this paper, we have tuned the giant AHE in CsV_3Sb_5 by applying hydrostatic pressure. We confirm that the AHE is strongly correlated with the CDW order even under pressure. In addition, a positive anomalous Hall resistivity signal suddenly emerges below 35 K at 0.75 GPa, which could be related to the Fermi surface reconstruction and/or Fermi energy shift under pressure. Our work demonstrates that CsV_3Sb_5 provides us an ideal platform to study the correlation between AHE and CDW in the kagome lattice system.

2. Methods

The CsV_3Sb_5 single crystals were grown using a self-flux method similar to the previous reports.[14] In order to prevent the reaction of Cs with air and water, all the preparation processes were performed in an argon glovebox. After reaction in the furnace, the as-grown CsV_3Sb_5 single crystals are stable in the air. The excess flux was removed using ethanol and millimeter-sized single crystal can be obtained. XRD data were collected at room temperature by using an x-ray diffractometer (SmartLab-9, Rikagu) with Cu K_α radiation. Electrical transport measurements were carried out in a Quantum Design PPMS-14T system. The longitudinal resistance and Hall resistance were simultaneously measured with standard six-probe Hall bar geometry. Hydrostatic pressure was established in a piston-cylinder cell (PCC) with Daphne 7373 oil used as the pressure transmitting medium. The pressure values in PCC were calibrated by measuring the superconducting transition temperature of pure tin.

3. Results and discussion

We first checked the quality of the as-grown CsV_3Sb_5 single crystals under ambient pressure, with results summarized in Fig. 1. Figure 1(b) displays the x-ray diffraction (XRD) pattern of a CsV_3Sb_5 single crystal. Only (00l) diffraction peaks can be detected which indicates the as-grown single crystal having a (00l) preferred orientation. The lattice constant c is 9.308 Å, being consistent with previous report.[13] Figure 1(c) displays the temperature dependence of resistivity of the sample at ambient pressure which shows T_C around 2.7 K. The residual resistivity ratio (RRR) is 61, suggesting high quality of the sample. The kink around 94 K in the resistivity curve is associated with the CDW transition, similar to the previous result.[14]

Next, we systematically investigated the pressure effect on the AHE in quasi-2D kagome superconductor CsV_3Sb_5 under various pressures. To evaluate the pressure effect on the AHE of CsV_3Sb_5, we measured Hall resistivity $\rho_{xy}(H)$ at different temperatures under various pressures. Figure 2 shows Hall effects of CsV_3Sb_5 at various temperatures under pressure of 0.36 GPa. As shown in the inset of Fig. 2(a), the CDW transition temperature T^* can be suppressed to 83 K,

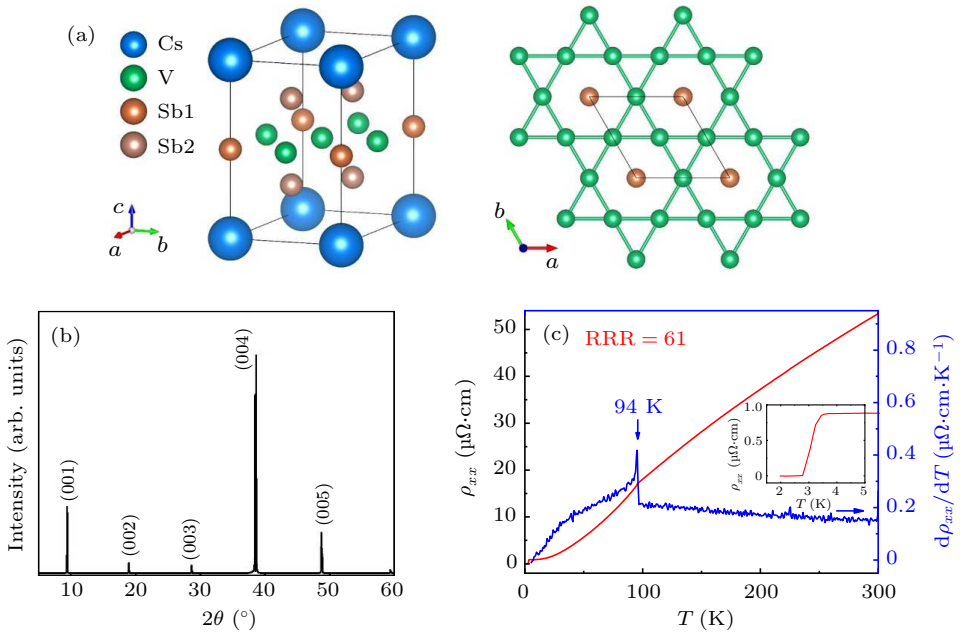


Fig. 1. Crystal structure of CsV_3Sb_5. The Cs, V, Sb1 and Sb2 atoms are presented as blue, green, puce and hazel balls, respectively. The vanadium sublattice forms perfect kagome lattice. (b) Single-crystalline x-ray diffraction pattern for the CsV_3Sb_5 single crystals. All the peaks can be well indexed with Miller indices (00l). (c) Temperature dependence of resistivity at ambient pressure. The arrows denote the CDW transitions at ∼ 94 K. The inset indicates the superconducting transition around 2.7 K.

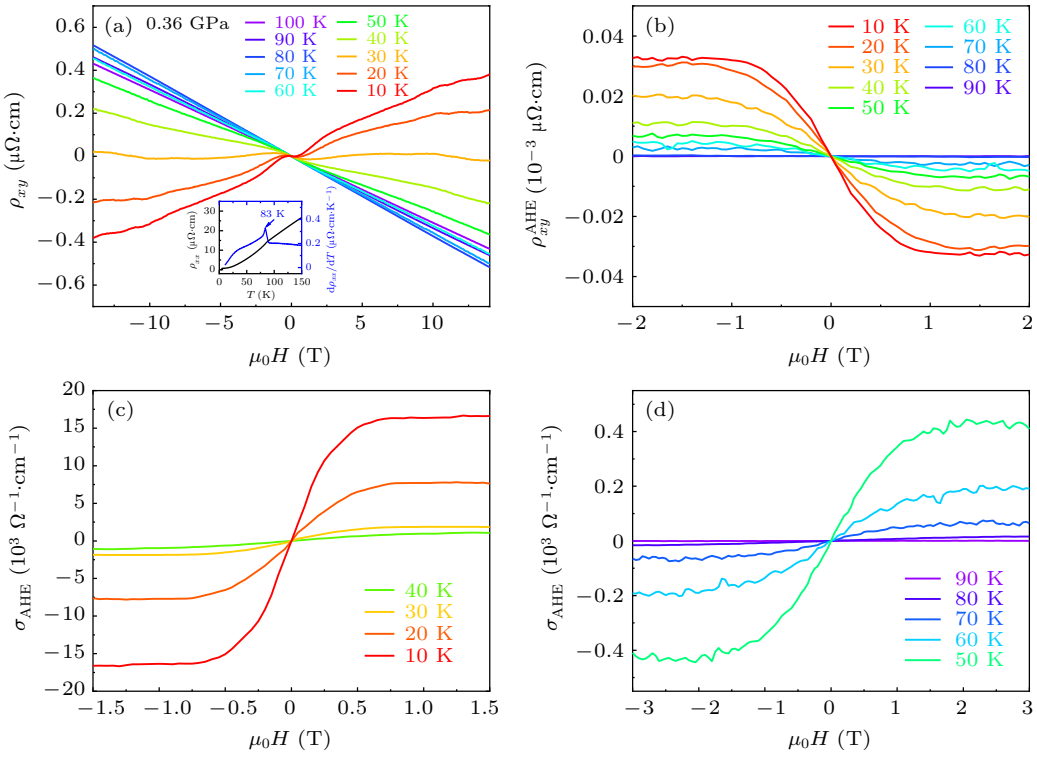


Fig. 2. Hall effects of CsV_3Sb_5 at 0.36 GPa. (a) The Hall resistivity as a function of field at various temperatures from 10 K to 100 K. The inset shows the temperature dependence of resistivity. T^* is suppressed to 83 K as determined from the derivative resistivity curve. (b) The extracted anomalous Hall resistivity taken by subtracting the local linear ordinary Hall background at various temperatures from 10 K to 90 K. AHE spontaneously emerges below T^*. (c) and (d) The extracted anomalous Hall conductivity at various temperatures.

consistent with the previous high-pressure results.[22] Similar to the case at ambient pressure,[19] ρ_{xy} exhibits a linear behavior at high temperature, indicating that the carrier density is dominated by one band. ρ_{xy} gradually deviates from the linear behavior below T^*, with the slope of high-field ρ_{xy} gradually decreasing and changing its sign around 30 K. Such behaviors could be attributed to the significant enhancement of hole mobility at low temperature. Similar to the ambient-pressure Hall data, an antisymmetric sideways "S" line shape is observed at low fields, which can be attributed to the AHE. We can extract $\rho_{xy}^{\rm AHE}$ by subtracting the local linear ordinary Hall term (typically from 1 T to 2 T at low temperature) as shown in Fig. 2(b). $\rho_{xy}^{\rm AHE}$ decreases with increasing temperature and persists up to the CDW transition temperature T^*. We can also obtain the Hall conductivity by inverting the resistivity matrix, $\sigma_{xy} = -\rho_{xy}/(\rho_{xx}^2 + \rho_{xy}^2)$. The anomalous Hall conductivity (AHC) $\sigma_{\rm AHE}$ is obtained by subtracting the local linear ordinary Hall conductivity background as shown in Figs. 2(c) and 2(d), which clearly shows the sudden appearance of the AHE below T^*.

To check the AHE evolution under pressure, we further increase the pressure above 0.7 GPa above which the superconductivity shows sudden suppression.[22,23] In Fig. 3(a) we plot the temperature variation of the resistivity ρ_{xx} of CsV_3Sb_5 at 0.75 GPa. The CDW transition temperature can be suppressed to $\sim$ 64 K as indicated by the arrow in the derivative of the ρ_{xx}–T curve. The ρ_{xy} at various temperatures is shown in Fig. 3(b). Unlike the case of the ambient pressure, the ρ_{xy} does not change sign at low temperatures, indicating a reduction of the hole contribution stemming from the change of Fermi surface pocket size or mobilities. By subtracting the local linear ordinary Hall term, we can obtain the $\rho_{xy}^{\rm AHE}$ as shown in Figs. 3(c) and 3(d). We find AHE emerges just below T^*, similar with the result measured at ambient pressure. More interestingly, a new AHE signal shows up below $\sim$ 35 K as shown in Fig. 3(d). This new AHE signal is positive which shows the opposite sign with the original one. The emergence of the positive anomalous Hall resistivity is possibly related to the Fermi surface reconstruction and/or Fermi energy shift under pressure. We can also extract the $\sigma_{\rm AHE}$ as shown in Figs. 3(e) and 3(f). $\sigma_{\rm AHE}$ also shows anomaly at low temperature which could be attributed to the other source of AHE. We notice that the new AHE has a saturation field smaller than the original one, indicating the different origins.

With further increasing the pressure, T^* can be suppressed to 49 K at 1.02 GPa as shown in the inset of Fig. 4(a). The Hall effect measurements at various temperatures are shown in Fig. 4(a). ρ_{xy} shows different behavior with that at 0.75 GPa at low temperature, which indicates that the Fermi surface may be rather sensitive to the pressure. The high-field nonlinear behavior of ρ_{xy} is related to the two-band ordinary Hall effect, which is similar to the ambient-pressure results.[18,19] The extracted ρ_{xy} decreases with increasing tem-

perature and persists up to the CDW transition temperature T^* as shown in Fig. 4(b). Similarly, the magnitude of the AHE monotonically decreases with increasing temperature until it is lost at around T^* as shown in Figs. 4(c) and 4(d). We notice that the positive anomalous Hall resistivity disappears, which is possibly due to the shift of the Fermi energy under pressure.

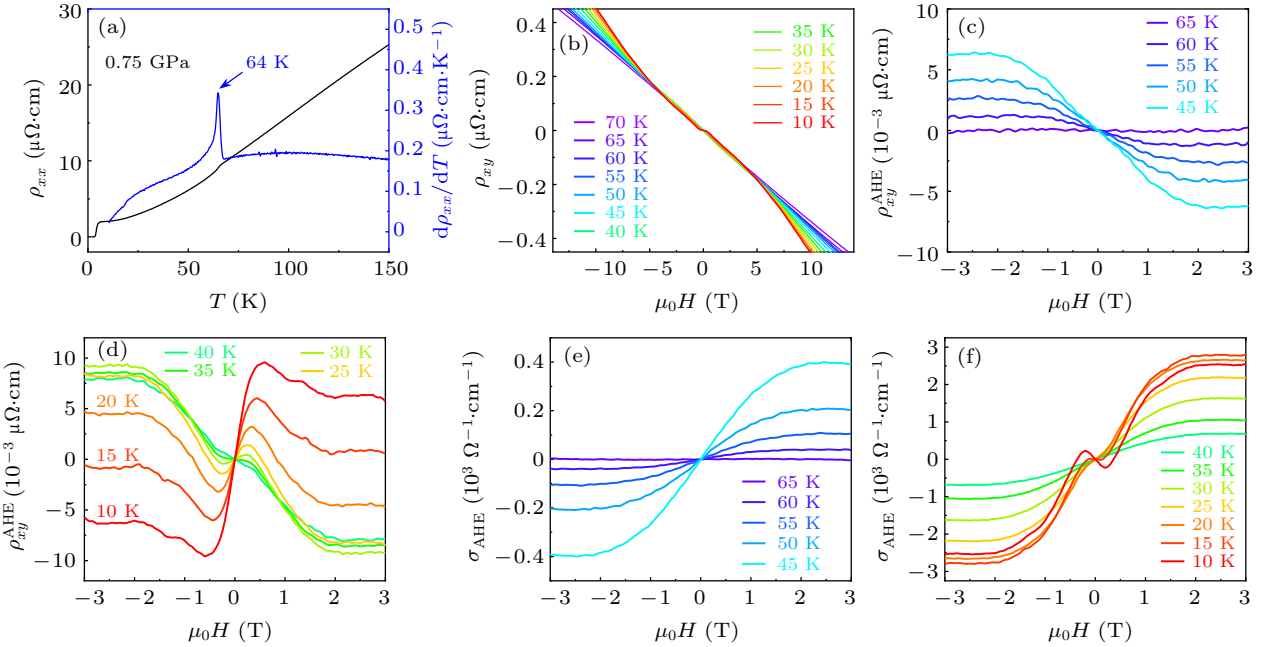


Fig. 3. Hall effects of CsV_3Sb_5 at 0.75 GPa. (a) Temperature dependence of the resistivity ρ_{xx} and the derivative resistivity $d\rho_{xx}/dT$. The CDW ordering temperature is indicated by arrows as $T^* \sim 64$ K. (b) Field dependent Hall resistivity ρ_{xy} at various temperatures from 10 K to 70 K. (c) and (d) The extracted anomalous Hall resistivity taken by subtracting the local linear ordinary Hall background at various temperatures from 10 K to 70 K. AHE spontaneously emerges below T^*. A positive anomalous Hall resistivity emerges below 35 K. (e) and (f) The extracted anomalous Hall conductivity at various temperatures.

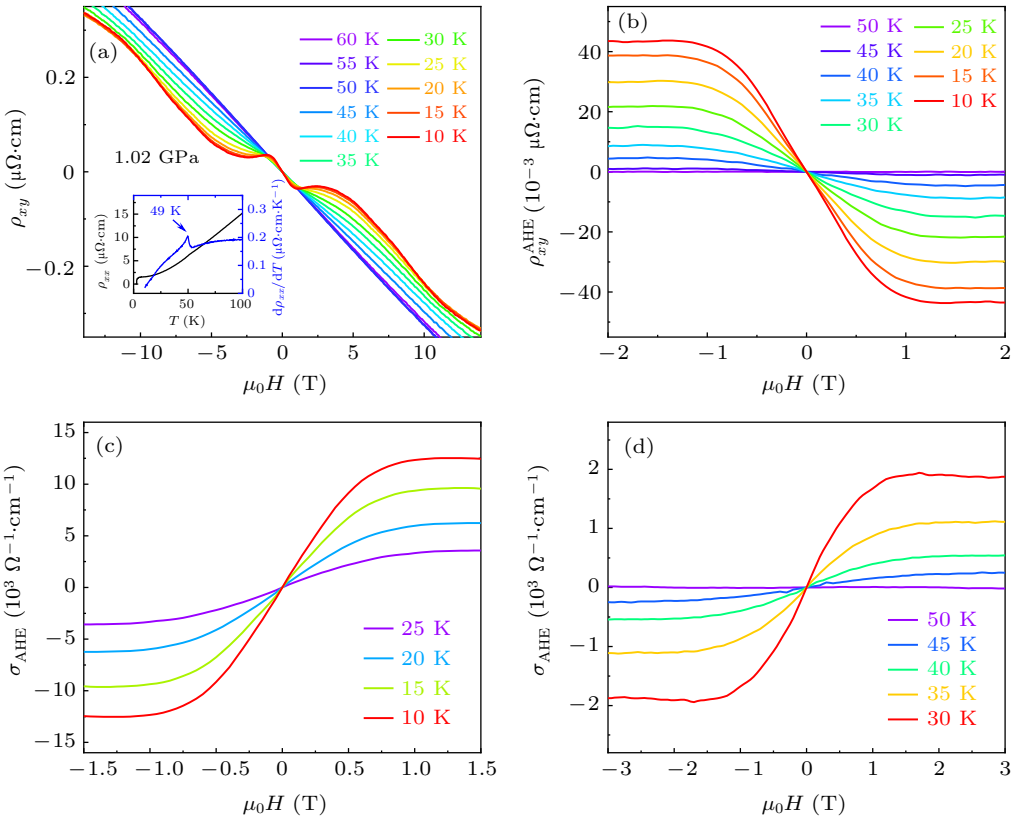


Fig. 4. Hall effects of CsV_3Sb_5 at 1.02 GPa. (a) The Hall resistivity at different temperatures. The inset shows the temperature dependence of resistivity and the derivative resistivity curve with a kink at $T^* \sim 49$ K. (b) The extracted anomalous Hall resistivity at various temperatures from 10 K to 60 K. AHE spontaneously emerges below T^*. (c) and (d) The extracted anomalous Hall conductivity at different temperatures.

Further increasing the pressure, T^* can be gradually suppressed. With pressure increasing to 1.78 GPa, T^* can be suppressed to 18 K as shown in Fig. S1 in the supplementary materials. The AHE also appears below T^*. By completely suppressing T^* above 2 GPa, AHE disappears.[19] Combing all the high-pressure Hall measurements, we can map out the phase diagram of CsV_3Sb_5 as shown in Fig. 5. The CDW is monotonically suppressed by elevating the pressure, and disappears at $\sim$ 2.0 GPa. The negative Hall resistivity persists up to the CDW transition temperature T^* even under pressure. Remarkably, the amplitude of the anomalous Hall resistivity suddenly decreases around 0.75 GPa, which is due to the abrupt emergence of the positive anomalous Hall resistivity. Such behavior can be strongly correlated with the new CDW order that develops above 0.7 GPa which will be detailed discussed below. At the meantime, the AHC also shows local minimum around 0.75 GPa, as shown in Fig. S2 in the supplementary materials.

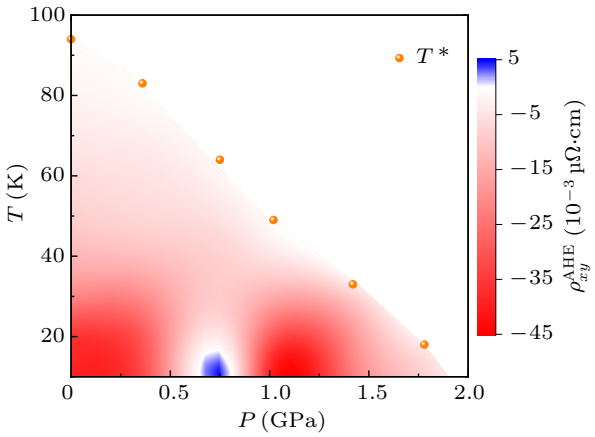


Fig. 5. The 2D color contour plot of the anomalous Hall resistivity ρ_{xy}^{AHE} as a function of P and T. Positive ρ_{xy}^{AHE} emerges around 0.75 GPa which is possibly due to the Fermi surface reconstruction or/and Fermi energy shift when the new CDW order develops.

Although the origin of the AHE in CsV_3Sb_5 is not well understood, our work unambiguously demonstrates that the negative anomalous resistivity immediately sets in below T^*, which indicates the intimate correlation between AHE and CDW. More interestingly, we observed a positive anomalous Hall resistivity emerges below 35 K at 0.75 GPa. The origin of AHE can be either intrinsic or extrinsic. Since the pressure is unlikely to sudden change the impurity, therefore, the extrinsic AHE should not change much under pressure. The intrinsic AHE is rather sensitive to the band structure and Fermi energy, both of them may be dramatically changed under pressure and could be the origins of the unusual AHE evolution under pressure. Previous high pressure works demonstrated that a new CDW order develops above 0.7 GPa, which would strongly suppress the superconductivity and lead to the intriguing two-dome superconductivity behavior.[22,23] The formation of the new CDW would naturally lead to the Fermi surface reconstruction, which could be one of the possibilities for the origin of the positive anomalous Hall resistivity. Such intrinsic AHE can be weakened when the Fermi energy slightly shifts at higher pressure. However, we can not figure out which band contributes to the intrinsic AHE from the current measurements. The band structure measurements are crucial to answer this question, though such measurements are rather difficult under pressure. Recently, the AHE is found to be tunable through proton intercalation in the CsV_3Sb_5 nanoflakes.[36] Peculiarly, the AHE change sign when the carrier is tuned from hole to electron,[36] similar to our high-pressure results. We propose that the AHE at ambient pressure is constituted by both extrinsic and intrinsic origins, by change the pressure, the Fermi energy shift may lead to the sign change of the intrinsic part of the AHE around 0.75 GPa. With further shifting the Fermi energy, the intrinsic AHE gradually vanishes and the extrinsic AHE dominates at higher pressure.

4. Conclusion

We systematically investigated the pressure effect of the AHE in CsV_3Sb_5. Our high-pressure transport measurements confirm the concurrence of AHE and CDW in the compressed CsV_3Sb_5. In addition, we observed that positive anomalous Hall resistivity emerges below 35 K at 0.75 GPa, such behavior can be attributed to the Fermi surface reconstruction and/or Fermi energy shift under pressure. Our results demonstrate that the intrinsic AHE in CsV_3Sb_5 can be easily tuned, making CsV_3Sb_5 an ideal platform to study the AHE and its correlation with CDW order.

Acknowledgments

This work was supported by the National Key Research and Development Program of China (Grant Nos. 2019YFA0704900 and 2017YFA0303001), the Anhui Initiative in Quantum Information Technologies (Grant No. AHY160000), the Science Challenge Project of China (Grant No. TZ2016004), the Key Research Program of Frontier Sciences, Chinese Academy of Sciences (CAS) (Grant No. QYZDYSSWSLH021), the Strategic Priority Research Program of the Chinese Academy of Sciences (Grant No. XDB25000000), the National Natural Science Foundation of China (Grants Nos. 11888101 and 11534010), the Collaborative Innovation Program of Hefei Science Center, CAS (Grant No. 2020HSC-CIP014), and the Fundamental Research Funds for the Central Universities, China (Grant No. WK3510000011).

References

[1] Nagaosa N, Sinova J, Onoda S, MacDonald A H and Ong N P 2010 *Rev. Mod. Phys.* **82** 1539

[2] Smit J 1958 *Physica* **24** 39
[3] Berger L 1970 *Phys. Rev. B* **2** 4559
[4] Nagaosa N 2006 *J. Phys. Soc. Jpn.* **75** 042001
[5] Xiao D, Chang M C and Niu Q 2010 *Rev. Mod. Phys.* **82** 1959
[6] Haldane F D M 2004 *Phys. Rev. Lett.* **93** 206602
[7] Taguchi Y, Oohara Y, Yoshizawa H, Nagaosa N and Tokura Y 2001 *Science* **291** 2573
[8] Wang Q, Xu Y F, Lou R, Liu Z H, Li M, Huang Y B, Shen D W, Weng H M, Wang S C and Lei H C 2018 *Nat. Commun.* **9** 3681
[9] Liang T, Lin J J, Gibson Q, Kushwaha S, Liu M H, Wang W D, Xiong H Y, Sobota J A, Hashimoto M, Kirchmann P S, Shen Z X, Cava R J and Ong N P 2018 *Nat. Phys.* **14** 451
[10] Suzuki T, Chisnell R, Devarakonda A, Liu Y T, Feng W, Xiao D, Lynn J W and Checkelsky J G 2016 *Nat. Phys.* **12** 1119
[11] Smit J 1955 *Physica* **21** 877
[12] Miyasato T, Abe N, Fujii T, Asamitsu A, Onoda S, Onose Y, Nagaosa N and Tokura Y 2007 *Phys. Rev. Lett.* **99** 086602
[13] Ortiz B R, Gomes L C, Morey J R, Winiarski M, Bordelon M, Mangum J S, Oswald L W H, Rodriguez-Rivera J A, Neilson J R, Wilson S D, Ertekin E, McQueen T M and Toberer E S 2019 *Phys. Rev. Mater.* **3** 094407
[14] Ortiz B R, Teicher S M L, Hu Y, Zuo J L, Sarte P M, Schueller E C, Abeykoon A M M, Krogstad M J, Rosenkranz S, Osborn R, Seshadri R, Balents L, He J F and Wilson S D 2020 *Phys. Rev. Lett.* **125** 247002
[15] Ni S L, Ma S, Zhang Y H, Yuan J, Yang H T, Lu Z Y W, Wang N N, Sun J P, Zhao Z, Li D, Liu S B, Zhang H, Chen H, Jin K, Cheng J G, Yu L, Zhou F, Dong X L, Hu J P, Gao H J and Zhao Z X 2021 *Chin. Phys. Lett.* **38** 057403
[16] Ortiz B R, Sarte P M, Kenney E M, Graf M J, Teicher S M L, Seshadri R and Wilson S D 2021 *Phys. Rev. Mater.* **5** 034801
[17] Yin Q W, Tu Z J, Gong C S, Fu Y, Yan S H and Lei H C 2021 *Chin. Phys. Lett.* **38** 037403
[18] Yang S Y, Wang Y J, Ortiz B R, Liu D F, Gayles J, Derunova E, Gonzalez-Hernandez R, Smejkal L, Chen Y L, Parkin S S P, Wilson S D, Toberer E S, McQueen T and Ali M N 2020 *Sci. Adv.* **6** eabb6003
[19] Yu F H, Wu T, Wang Z Y, Lei B, Zhuo W Z, Ying J J and Chen X H 2021 *Phys. Rev. B* **104** L041103
[20] Jiang Y X, Yin J X, Denner M M, Shumiya N, Ortiz B R, Xu G, Guguchia Z, He J, Hossain M S, Liu X, Ruff J, Kautzsch L, Zhang S S, Chang G, Belopolski I, Zhang Q, Cochran T A, Multer D, Litskevich M, Cheng Z J, Yang X P, Wang Z, Thomale R, Neupert T, Wilson S D and Hasan M Z 2021 *Nat. Mater.* **20** 1353
[21] Feng X, Jiang K, Wang Z and Hu J 2021 *Sci. Bull.* **66** 1384
[22] Yu F H, Ma D H, Zhuo W Z, Liu S Q, Wen X K, Lei B, Ying J J and Chen X H 2021 *Nat. Commun.* **12** 3645
[23] Chen K Y, Wang N N, Yin Q W, Gu Y H, Jiang K, Tu Z J, Gong C S, Uwatoko Y, Sun J P, Lei H C, Hu J P and Cheng J G 2021 *Phys. Rev. Lett.* **126** 247001
[24] Zhang Z Y, Chen Z, Zhou Y, Yuan Y F, Wang S Y, Wang J, Yang H Y, An C, Zhang L L, Zhu X D, Zhou Y H, Chen X L, Zhou J H and Yang Z R 2021 *Phys. Rev. B* **103** 224513
[25] Wang Q, Kong P, Shi W, Pei C, Wen C, Gao L, Zhao Y, Yin Q, Wu Y and Li G 2021 *Adv. Mater.* **33** 2102813
[26] Chen X, Zhan X H, Wang X J, Deng J, Liu X B, Chen X, Guo J G and Chen X L 2021 *Chin. Phys. Lett.* **38** 057402
[27] Zhao C C, Wang L S, Xia W, Yin Q W, Ni J M, Huang Y Y, Tu C P, Tao Z C, Tu Z J, Gong C S, Lei H C, Guo Y F, Yang X F and Y L S 2021 arXiv: 2102.08356
[28] Sun Z L, Peng K L, Cui J H, Zhu C S, Zhuo W Z, Wang Z Y and Chen X H 2021 *Phys. Rev. B* **103** 085116
[29] Chen X, Wang M, Gu C, Wang S, Zhou Y, An C, Zhou Y, Zhang B, Chen C, Yuan Y, Qi M, Zhang L, Zhou H, Zhou J, Yao Y and Yang Z 2019 *Phys. Rev. B* **100** 165145
[30] Liu Z Y, Zhang T, Xu S X, Yang P T, Wang Q, Lei H C, Sui Y, Uwatoko Y, Wang B S, Weng H M, Sun J P and Cheng J G 2020 *Phys. Rev. Mater.* **4** 044203
[31] Wang X, Li Z, Zhang M, Hou T, Zhao J, Li L, Rahman A, Xu Z, Gong J, Chi Z, Dai R, Wang Z, Qiao Z and Zhang Z 2019 *Phys. Rev. B* **100** 014407
[32] Reis R D d, Ghorbani Zavareh M, Ajeesh M O, Kutelak L O, Sukhanov A S, Singh S, Noky J, Sun Y, Fischer J E, Manna K, Felser C and Nicklas M 2020 *Phys. Rev. Mater.* **4** 051401
[33] Singh C, Singh V, Pradhan G, Srihari V, Poswal H K, Nath R, Nandy A K and Nayak A K 2020 *Phys. Rev. Res.* **2** 043366
[34] Lee M, Kang W, Onose Y, Tokura Y and Ong N P 2009 *Phys. Rev. Lett.* **102** 186601
[35] Akiba K, Iwamoto K, Sato T, Araki S and Kobayashi T C 2020 *Phys. Rev. Res.* **2** 043090
[36] Zheng G L, Chen Z, Tan C, Wang M Y, Zhu X D, Albarakati S, Algarni M, Partridge J, Farrar L, Zhou J H, Ning W, Tian M L, Fuhrer M S and Wang L 2021 arXiv: 2109.12588v1